Analysis of the Valence X-Ray Photoelectron Spectra of Eight $(-CH_2-CHR-)_n$ and Two $(-CH_2-C(CH_3)R-)_n$ Polymers by the Semi-Empirical HAM/3 MO Method Using the Trimer Model Molecules $H-(-CH_2-CHR-)_3-H$ and $H-(-CH_2-C(CH_3)R-)_3-H$

Masayuki AIDA, Yasuo KANEDA, Naoya KOBAYASHI, Kazunaka ENDO,* and Delano P. CHONG*,†
Tsukuba Research Laboratory, Mitsubishi Paper Mills, Ltd., 46 Wadai, Tsukuba, Ibaraki 300-42
† Department of Chemistry, University of British Columbia, 2036 Main Mall, Vancouver, B.C., V6T 1Z1 Canada
(Received June 13, 1994)

The valence X-ray photoelectron spectra of ten polymers $[(-CH_2-CHR-)_n$ (R=C_6H_5, OCH_3, $COCH_3$, COOH, $COOCH_3$, $OCOCH_3$, $CONH_2$, C_4H_6NO (*N*-vinylpyrrolidone)) and $(-CH_2-C(CH_3)R-)_n$ (R=$COOCH_3$ and $CONH_2$)] were analyzed by a semi-empirical HAM/3 MO method using trimer model molecules [$H-(-CH_2-CHR-)_3-H$ (R=C_6H_5, OCH_3, $COCH_3$, COOH, $COOCH_3$, $OCOCH_3$, $CONH_2$, and C_4H_6NO (*N*-vinylpyrrolidone) and $H-(-CH_2-C(CH_3)R-)_3-H$ (R=$COOCH_3$ and $CONH_2$)], respectively. The calculated Al $K\alpha$ photoelectron spectra were obtained using Gaussian functions of a fixed approximate linewidth (0.10 I_k; $I_k=I'_k-\Delta W$, where I'_k is the vertical ionization potential of each MO and ΔW is an approximate shift to account for the work-function effects. We assumed that ΔW corresponds to the shift that we must apply before we could compare the calculated spectrum for a single model molecule with the observed spectrum for the solid. The theoretical spectra showed good agreement with the spectra of the polymers, as observed between 0—40 eV.

After Åsbrink et al.[1—3] proposed a semi-empirical hydrogenic atoms in molecules (HAM/3) molecular-orbital (MO) method, based on Slater's concepts,[4—6] the MO method was studied and extended by Chong[7,8] to interpret different kinds of electron spectroscopy, such as Auger electron spectra,[9] valence-electron shake-up satellites,[10] core-electron shake-up spectra,[11] X-ray photoelectron spectra (XPS) with intensity[12] and X-ray emission spectra.[8,13] In the present study, our aim was to interpret the experimental valence XPS of polymers by HAM/3 calculations using the trimer model.

The XPS from monochromatized X-ray radiation has become a powerful tool for studying the electronic structure of polymers. This technique provides precise information concerning the core-level binding energies and linewidths, and records the distribution of the valence electronic levels, which constitute a real and unique

Table 1. Relative Photoionization Cross-Section (PICS) of Each Atomic Orbital for H,C, N, and O Atoms (Relative to C2s)

Atomic orbital	Al $K\alpha$ (Nefedov et al.[26])
H 1s	0.0093
C 2s	1.0000
2p	0.0324
N 2s	1.8210
2p	0.0902
O 2s	2.9480
2p	0.2029

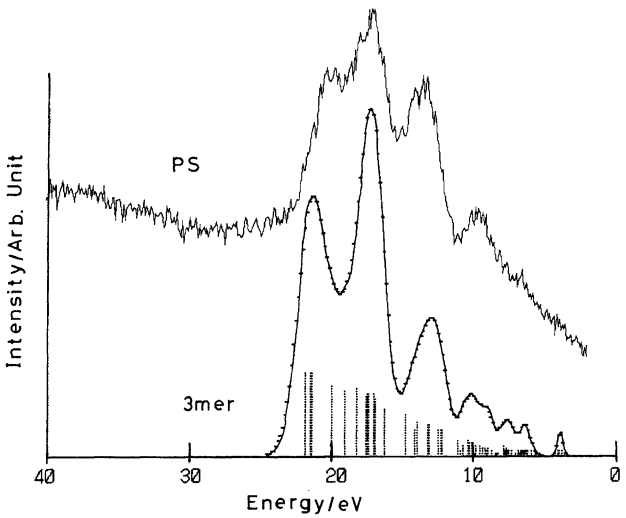

Fig. 1. Valence XPS of PS with the simulated spectrum and with the spectral pattern of the trimer model molecule as calculated using HAM/3.

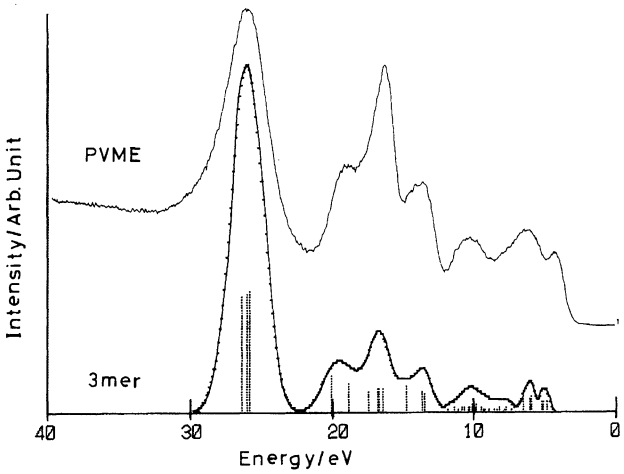

Fig. 2. Valence XPS of PVME with the simulated spectrum and with the spectral pattern of the trimer model molecule using HAM/3.

Table 2. Observed Peaks, VIP, Main AO PICS, Orbital Nature, and Functional Group for Valence XPS of PS [(The Gap between Observed and Calculated VIPs)=5.0 eV]

Peak (eV)	VIP (eV)	Main AO PICS	Orbital nature[b)]	Functional group
20.0	(26.81;26.44;26.30)	C2s	$s\sigma$(C2s–2s)–B	$-C_6H_5$,–C(main chain)
(19—23)[a)]	(24.92;24.07)	C2s	$s\sigma$(C2s–2s)–B	–C(main chain),$-C_6H_5$
17.0	(23.18;22.55;22.48;	C2s	$s\sigma$(C2s–2s)–B	$-C_6H_5$
(15.5—19)[a)]	22.42;22.04)			
	(21.89;21.31)	C2s	$s\sigma$(C2s–2s)–B	–C(main chain),$-C_6H_5$
13.5	(19.80;19.13;18.94;	C2s	$s\sigma$(C2s–2s)–B	–C(main chain),$-C_6H_5$
(12—15.5)[a)]	18.27;18.15;18.12)	C2s	$p\sigma$(C2s–2p)–B	$-C_6H_5$
	(17.52;17.28;17.22)	C2s	$p\sigma$(C2s–2p)–B	$-C_6H_5$,–C(main chain)
10.0	(15.42;15.27;	C2p	$p\sigma$(C2p–H1s)–B	–C(main chain),$-C_6H_5$
	15.11;14.81)	C2p	$p\sigma$(C2p–H1s)–B	$-C_6H_5$,–C(main chain)
(3.5—12)[a)]	Many adjacent levels			
	(16.09;15.96;15.77)	C2p	$p\sigma$(C2p–H1s)–B	$-C_6H_5$,–C(main chain)
	14.6—13.7	C2p	$p\sigma$(C2p–H1s)–B	$-C_6H_5$,–C(main chain)
	(13.4—8.9)	{C2p	$p\sigma$(C2p–H1s)–B	$-C_6H_5$,–C(main chain);
		C2p	$p\pi_p$(C2p–2p)–B	$-C_6H_5$,–C(main chain)}

a) Shows the peak range. b) π_p indicates the pseudo π orbitals of the CH_2 groups. B and NB mean bonding and non bonding, respectively. (C2s–2s), (C2s–2p) mean (C2s–C2s), (C2s–C2p), respectively.

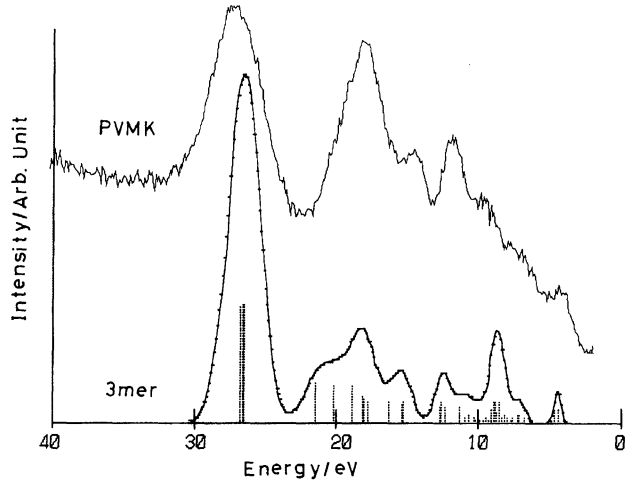

Fig. 3. Valence XPS of PVMK with the simulated spectrum and with the spectral pattern of the trimer model molecule using HAM/3.

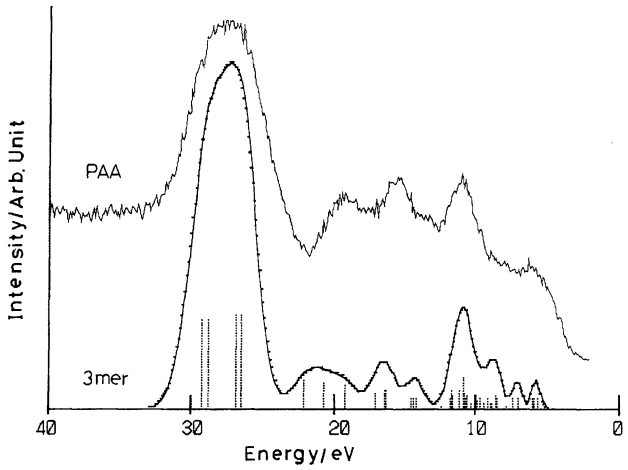

Fig. 4. Valence XPS of PAA with the simulated spectrum and with the spectral pattern of the trimer model molecule using HAM/3.

fingerprint of a compound. Some XPS valence-level studies[14—18] of simple model oligomers and saturated hydrocarbons showed that information concerning the conformational dependency of the polymer structure can be obtained through a spectral simulation using MO calculations.

In previous papers[19—22] we presented a new approach to interpretating the XPS core and valence level spectra of some polymers by ab initio and semi-empirical MO methods using the n-mer model and one-dimensional polymers, respectively. We ascertained that XPS is too insensitive to give spectra which depend on the stereoisomers of polymers. Furthermore, we examined a simulation of XPS for six representative polymers $[(-CH_2-CHR-)_n$ (R=H, CH_3, OH, and F), $(-CH_2-CH_2-NH-)_n$ and $(-CH_2-CH_2-O-)_n]$ using the n-mer (n=2 to 5) model molecules. The results[22] suggested that the observed spectra can be simulated by considering the trimer model molecules. Thus, in the present study we also used syndiotactic model molecules for eight $(-CH_2-CHR-)_n$ and two $(-CH_2-C(CH_3)R-)_n$ polymers to analyze the XPS spectra of the polymers by the HAM/3 method.

The present paper discusses a theoretical simulation for the valence photoelectron spectra of the polymers by the MO method using the model molecules. The simulation was obtained by taking the vertical ionization potential (VIP) for each MO from the HAM/3 calculation and using the Gelius model[23] for the molecular photoionization cross-section (PICS). The theoretical spectra were constructed from a superposition of the peaks centered at the calculated VIPs. The peak shape was represented by a Gaussian function. A good fit be-

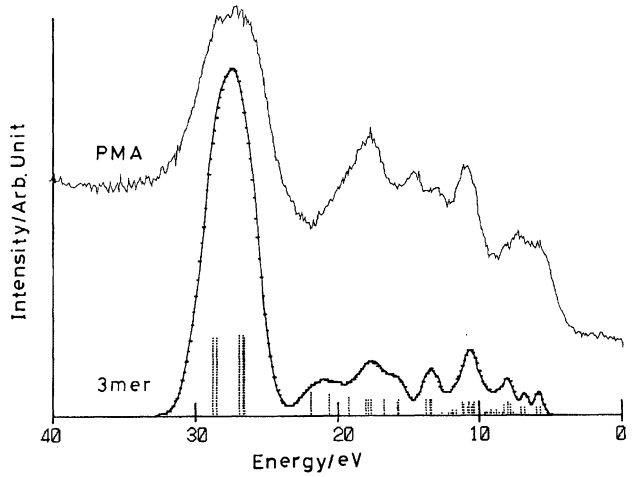

Fig. 5. Valence XPS of PMA with the simulated spectrum and with the spectral pattern of the trimer model molecule using HAM/3.

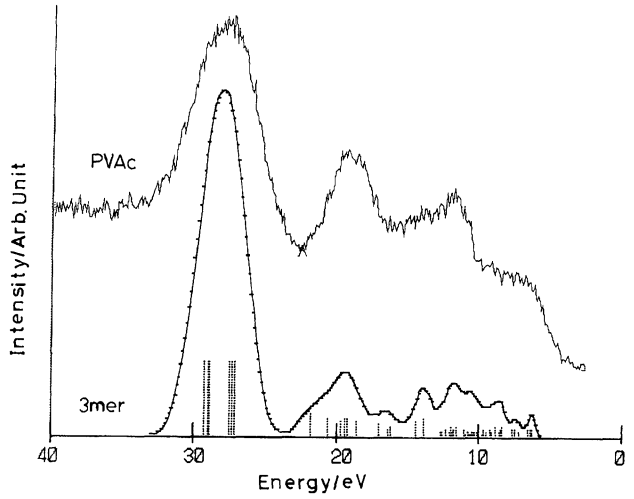

Fig. 6. Valence XPS of PVAc with the simulated spectrum and with the spectral pattern of the trimer model molecule using HAM/3.

tween the theoretical and the observed spectra enabled us to determine which region of each spectrum of the polymers is due to the PICS for any atomic orbitals of the constituent elements of the functional groups.

Theoretical Background

When one uses the diffuse ionization model[2] in the HAM/3 method, the eigenvalues give the VIP directly.

Because calculations for single molecules based on the trimer model are compared to experiments on a solid, we must shift each computed VIP I'_k by a quantity ΔW as $I_k = I'_k - \Delta W$.[24] This ΔW is given by $(W_{sp} - W_{sa})$, where W_{sp} is the work function of the spectrometer and W_{sa} is the gap between the vacuum and the Fermi levels of the sample.[24] In this work, approximate values of ΔW ranging from 3 to 5 eV were chosen to the nearest 0.5 eV by an inspection in order to provide the best agreement concerning the location of the main features

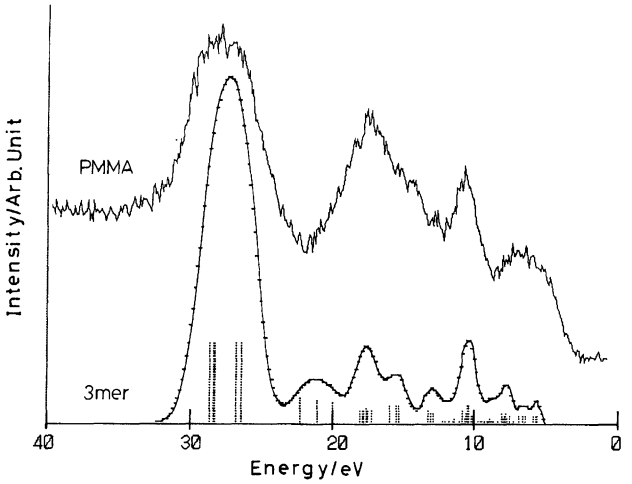

Fig. 7. Valence XPS of PMMA with the simulated spectrum and with the spectral pattern of the trimer model molecule using HAM/3.

of the simulated spectrum.

Gelius–Siegbahn[23] proposed a model to explain the intensities of the photoelectron lines of molecules. In the LCAO-MO approximation, the PICS of molecular orbitals is related to the cross section for the ionization of the atomic orbitals and the atomic populations in the molecular orbitals,

$$\sigma_j^{MO} = \sum_{A\lambda} P_{A\lambda j} \sigma_{A\lambda}^{AO}, \quad (1)$$

where the coefficient ($P_{A\lambda j}$) is the gross atomic population on atom A from AO λ in MO j, and $\sigma_{A\lambda}^{AO}$ is the relative PICS of AO Aλ.

The model molecules [H–(–CH_2–CHR–)$_3$–H (R= C_6H_5, OCH_3, $COCH_3$, COOH, $COOCH_3$, $OCOCH_3$, $CONH_2$, C_4H_6NO (*N*-vinylpyrrolidone)) and H–(–CH_2–$C(CH_3)R$–)$_3$–H (R=$COOCH_3$ and $CONH_2$)] were calculated by the semi-empirical HAM/3 program (a new version extended by Chong[12]). For the geometry of the molecules, we used the optimized structures from the semi-empirical AM1 (version 6.0) method.[25]

In the HAM/3 program, we can obtain the semi-empirical relative PICS of the Gelius model as well as the ab initio relative PICS for both Mg $K\alpha$ (1253.6 eV) and Al $K\alpha$ (1486.6 eV) radiation of Nefedov et al.[26] based on the Hartree–Fock–Slater methods. The atomic PICS, as described by Nefedov, was obtained under the assumption that the electrostatic atomic field was spherically symmetrical. In the present study we used the relative PICS values for each AO given in Table 1.

In order to simulate the valence XPS of polymers theoretically, we constructed from a superposition of peaks centered on the VIPs, I'_k. The peak shape is represented by the following Gaussian function:

$$f(x) = A(k) \exp\{-B(k)(x - I_k)\}^2, \quad (2)$$

where the intensity ($A(k)$) is estimated from the relative PICS for Al $K\alpha$ radiation. For $B(k)$, we used the

Table 3. Observed Peaks, VIP, Main AO PICS, Orbital Nature, and Functional Group for Valence XPS of PVME [(The Gap between Observed and Calculated VIPs)=4.5 eV]

Peak (eV)	VIP (eV)	Main AO PICS	Orbital nature[b)]	Functional group
26.5	(30.86;30.52;30.38)	O2s(0.94);C2s(0.06)	sσ(O2s–C2s)–B	–O–C–,–O–CH_3
(23—31)[a)]				
19.5	(24.59;23.39)	C2s(0.8);O2s(0.2)	sσ(C2s–C2s,O2s)–B	–C–(main chain),–C–O
(18.5—22)[a)]				
16.5	(21.30;21.20;20.94)	C2s(0.5);O2s(0.5)	sσ(C2s–O2s)–B	H_3C–O,–C–(main chain)
(15.5—18.5)[a)]	22.00	C2s	pσ(C2s–O2p)–B	–C–(main chain),H_3C–O
14.0	(19.34;18.16;18.05)	C2s(0.7);O2s(0.3)	sσ(C2s–O2s)–B	–C–O–,–CH_3
(12.5—15.5)[a)]				
10.5	(14.77;14.61;14.32)	O2p(0.5);C2p(0.5)	pσ(O,C2ps–C2p,2s)–B	–O–CH_3,–O–C–
(9—12)[a)]	Many adjacent levels	O2p(0.5),C2p(0.5)	pσ,pπ(C,O2p–2p)–B	–O–C–,–O–CH_3
			pσ(C2p–H1s)–B	–CH–,–CH_3
6.5	(11.01;10.58;10.44)	O2p(0.5);C2p(0.5)	pπ(O2p,C2p–C2p)–B	–O–C–,–O–CH_3
(5—9)[a)]				
4.5	(9.78;9.62;9.38)	O2p(0.9);C2p(0.1)	pπ(lone-pair)–NB	–O–
(3.5—5)[a)]				

a) Shows the peak range. b) B and NB mean bonding and nonbonding, respectively. (C,O2s–2p) means (C2s–C2p) and (O2s–O2p), (C2p, O2p–C2p) denotes (C2p–C2p) and (O2p–C2p), and so on.

Table 4. Observed Peaks, VIP, Main AO PICS, Orbital Nature and Functional Group for Valence XPS of PVMK [(The Gap between Observed and Calculated VIPs)=4.5 eV]

Peak (eV)	VIP (eV)	Main AO PICS	Orbital nature[b)]	Functional group
27.0	(31.26;31.06;30.97)	O2s(0.9);C2s(0.1)	sσ,pσ(O2s–C2s,C2p)–B	–C=O
(23—31)[a)]				
18.0	(23.36;22.64;	C2s	sσ(C2s–C2s,O2s)–B	–CO–CH_3,–C–(main chain)
(16—22)[a)]	22.50;22.21)			
	(25.93;24.61)	C2s(0.2);O2s(0.2)	sσ(C2s–C2s,O2s)–B	–C–(main chain),–C=O
15.0	(20.75;19.88;19.73)	C2s	sσ(C2s–2s,H1s)–B	–C–(main chain)
(13.5—16)[a)]				
12.0	(17.19;17.05;16.83)	C2s(0.8);O2s(0.2)	pσ(C,O2s–C,O2p)–B	–C–CO–,–CO–CH_3
(11—13.5)[a)]	(15.81;15.44;15.15)	C2s	pσ(C2p–C2s,H1s)–B	–C–(main chain),CH_3
(3—11)	Many adjacent levels			
	(14.8—13.8)	C2p	pσ(C2p–C2p,H1s)–B	–C–(main chain),CH_3
	(13.6—11.3)	C2p,O2p	{pσ(C,O2p–2p;C2p–H1s)–B	–C–CO,–CO–CH_3
			pπ(C2p,O2p–C2p)–B]	
4.5	(9.78;9.62;9.38)	O2p(0.9);C2p(0.1)	pπ(lone-pari)–NB	–C=O
(3.5—5.5)[a)]				

a) Shows the peak range. b) B and NB mean bonding and nonbonding, respectively. (C,O2s–2p) means (C2s–C2p) and (O2s–O2p), (C2p, O2p–C2p) denotes (C2p–C2p) and (O2p–C2p), and so on.

linewidth, $WH(k)=2(L_n/B(k))^{1/2}$. The linewidth was introduced for two reasons: (a) we were approximating the density of states by discrete MO levels, and (b) each state has a natural linewidth due to instrumental resolution, electronic relaxation processes, vibrational broadening and so on. By trial and error, we found that the simulated spectra had a reasonable appearance when we chose a simple form for the linewidth, such as

$$WH(k) = 0.10I_k, \tag{3}$$

for a trimer molecule.

Experimental

The experimental photoelectron spectra of six polymers were obtained on a Perkin–Elmer (model PHI 5400 MC ESCA) spectrometer, using monochromatized Al $K\alpha$ radiation. The spectrometer was operated at 600 W, 15 kV, and 40 mA. The photon energy was 1486.6 eV. A pass energy of 35.75 eV was employed for high-resolution scans in a valence-band analysis (range of 50 eV). The angle between the X-ray source and the analyzer was fixed at 45°. The spot size in the measurement was 3×1 mm.

The use of dispersion compensation yielded an instrumental resolution of 0.5 eV with a full width at half maximum on the Ag3d line of silver. Multiple-scan averaging on a multichannel analyzer was used for the valence-band region, although a very low photoelectron emission cross section was observed in this range.

We used commercially available polystyrene (PS) (Scientific Polymer Products, Inc.; M_w 280000), poly(methyl vinyl ether) (PVME) (Scientific Polymer Products,

Table 5. Observed Peaks, VIP, Main AO PICS, Orbital Nature and Functional Group for Valence XPS of PVAc [(The Gap between Observed and Calculated VIPs)=3.0 eV]

Peak (eV)	VIP (eV)	Main AO PICS	Orbital nature[b)]	Functional group
27.0	32.27;31.98;31.92	O2s(0.9),C2s(0.1)	sσ(O2s–C2s)–B	–O–
(23—32)[a)]	30.51;30.31;30.11	O2s	pσ(O2s–C2p)–B	O=C–
19.0	22.68;22.38;22.24	C2s	sσ(C2s–2s)–B	–C–(main chain)
(16—22)[a)]	24.78;23.58;21.55	C2s	sσ(C2s–2s)–B	–C–(main chain),–CH_3
	20.01;19.37;19.19	C2s(0.8),O2p(0.2)	pσ(C2s–O2p)–B	–C–O–C=O
12.0	(14.96—14.60)	O2s,O2p,C2s,C2p	pσ(O,C2p–2p)–B	–O–C–,O=C–
(10—15)[a)]	17.40;16.91;16.84	O2s,O2p,C2s,C2p	pσ(O,C2p–2p)–B	–O–C–,O=C–
	(15.70—15.05)	O2p,C2p	pσ,pπ(C,O2p–2p)–B	{–C–C–(main chain), –C–O–, O=C–}
(3—8)[a)]	below 14.01 eV Many adjacent levels			
	(14.01—11.39)	O2p,C2p	{pπ(O2p,C2p–C2p)–B; pσ(C2p–H1s)–B}	–O–,O=,–C– –CH_3
	10.67;10.44;10.16	O2p	pπ(lone pair)–NB	O=,–O–
	9.48;9.34;9.21	O2p	pπ(lone pair)–NB	O=,–O–

a) Shows the peak range. b) B and NB mean bonding and nonbonding, respectively. (C,O2s–2p) means (C2s–C2p) and (O2s–O2p), (C2p, O2p–C2p) denotes (C2p–C2p) and (O2p–C2p), and so on.

Table 6. Observed Peaks, VIP, Main AO PICS, Orbital Nature and Functional Group for Valence XPS of PMA [(The Gap between Observed and Calculated VIPs)=3.5 eV]

Peak (eV)	VIP (eV)	Main AO PICS	Orbital nature[b)]	Functional group
27.5	32.30;31.97;31.96	O2s(0.9);C2s(0.1)	sσ(O2s–C2s)–B	–O–,O=C
(23—33)[a)]	30.42;30.13;30.08	O2s(0.97);C2s(0.03)	pσ(O2s–C2p)–B	O=C,–O–
18.0	21.49;21.32;21.13	C2s(0.8);O2s(0.15)	sσ(C2s–C,O2s)–B	–O–C,–CH_3
(17—22)[a)]	25.40;24.07;22.74	C2s	sσ(C2s–C2s)–B	–C–(main chain),–CH_3
	20.21;19.31;19.20	C2s	sσ(C2s–C2s)–B	–C–(main chain),–CH_3
15.0	17.25;17.01;16.92	C2s(0.7);O2s,O2p	pσ(C2s–C,O2p)–B	–C–(main chain),–O–CO–
(12.5—17)[a)]	(16.16—15.16)	O2p(0.5);C2p(0.5)	pσ,pπ(O,C2p–2p)–B	–O–C=O–
11.0	(14.68—13.48)	O2s(0.5);O2p(0.3)	pσ(O,C2p–O2p,2s)–B	–O–CO–,–C–(main chain)
(9.5—12.5)[a)]	Many adjacent levels			
	(13.16—11.84)	C2p(0.7),O2p(0.3)	pσ,pπ(O,C2p–2p)–B	–O–C=O
(4—9.5)[a)]	11.74;11.48;11.34	O2p(0.7);C2p(0.3)	pπ(lone pair)–NB	O=C–,–O–
	10.56;10.31;10.28	O2p	pπ(lone pair)–NB	O=,–O–
	9.50;9.44;9.17	O2p	pπ(lone pair)–NB	O=,–O–

a) Shows the peak range. b) B and NB mean bonding and nonbonding, respectively. (C,O2s–2p) means (C2s–C2p) and (O2s–O2p), (C2p, O2p–C2p) denotes (C2p–C2p) and (O2p–C2p), and so on.

Inc.), poly(methyl vinyl ketone) (PVMK) (Scientific Polymer Products, Inc.; M_w 500000), polyacrylic acid (PAA) (Scientific Polymer Products, Inc.; M_w 4000000), poly(methyl acrylate) (PMA) (Scientific Polymer Products, Inc.; M_w 30700), poly(vinyl acetate) (PVAc) (Aldrich Chemical Co., Inc.; M_w 194800), polyacrylamide (PAM) (Aldrich Chemical Co., Inc.), poly(*N*-vinylpyrrolidone) (PNVP) (ICI Chemical Co., Inc.; M_w 40000), poly(methyl methacrylate) (PMMA) (Aldrich Chemical Co., Inc.; M_w 93300) and polymethacrylamide (PMAM) (Scientific Polymer Products, Inc.). Samples were prepared by cast-coating the polymer solution on an aluminium plate, while toluene, water, and chloroform were used for the (PS, PVME, PMA), (PAM, PNVP, PMAM), and (PAA, PVMK, PVAc, PMMA) polymers, respectively. A low-energy electron flood gun was used in order to avoid any charging effect on the surface of the sample. After obtaining an absolute calibration, the C1s line positions (285.0 eV) on the polymer films were accurately measured to serve as an energy reference for the polymers.

Results and Discussion

The vertical ionization potentials predicted by Koopmans' theorem are often too high (by approximately 8%). In contrast, the VIPs calculated by the HAM/3 method have an average absolute deviation of about 0.4 eV.[7,26)] Moreover, any incorrect assignment of the peaks in the photoelectron spectra by the HAM/3 method is extremely rare. Based on such performance, we have some confidence in the modeling of polymers by applying the HAM/3 method to the trimer model. The agreement between the simulated and observed XPS of polymers gives us further assurance about our interpretation of the different regions of the spectra.

(a) Valence XPS of PS Polymer. In Fig. 1, the

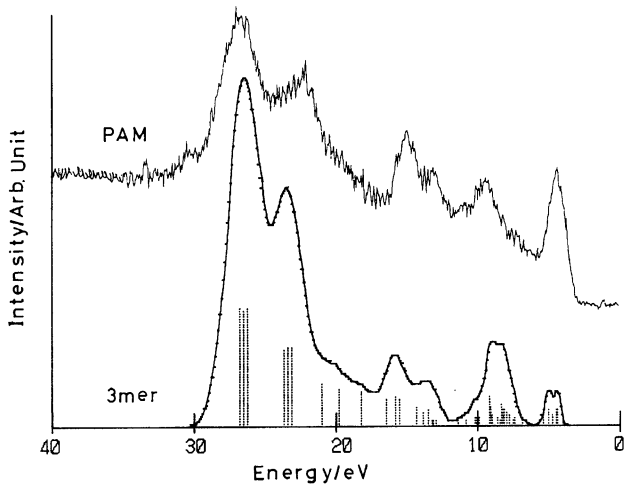

Fig. 8. Valence XPS of PAM with the simulated spectrum and with the spectral pattern of the trimer model molecule using HAM/3.

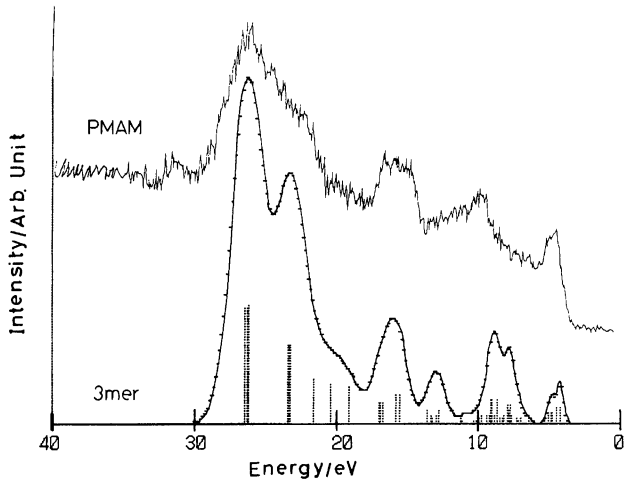

Fig. 10. Valence XPS of PMAM with the simulated spectrum and with the spectral pattern of the trimer model molecule using HAM/3.

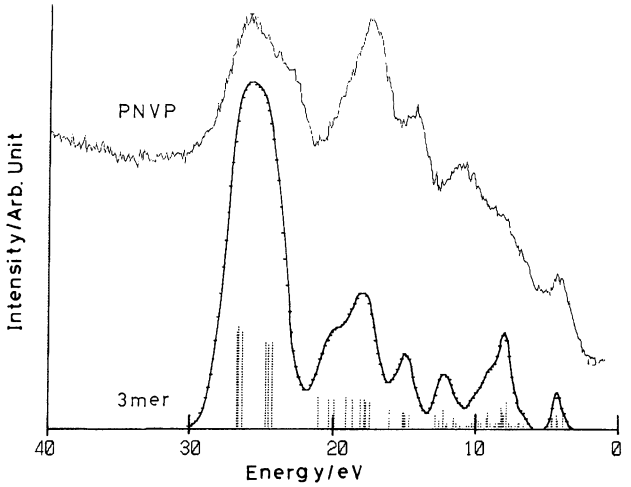

Fig. 9. Valence XPS of PNVP with the simulated spectrum and with the spectral pattern of the trimer model molecule using HAM/3.

simulated spectrum of PS with the spectral patterns is compared with the observed XPS. As mentioned earlier, the simulation used a Gaussian lineshape function for each MO with a model linewidth of Eq. 3 and $I_k = I'_k - \Delta W$. The simulated spectra using the trimer model is in good accordance with the observed spectra of the polymers. The shift due to work-function effects was estimated to be 5.0 eV for PS.

Table 2 shows the observed peaks, the VIPs, the main AO PICS, the orbital nature and the functional group for PS. The intense spectrum at around 17.0 eV (Fig. 1 and Table 2) corresponds to the VIP of an $s\sigma$(C2s–C2s)-bonding orbital, which results from the $-C_6H_5$ group. The peaks at around 14 and 20 eV for the polymers (in Fig. 1) are due to the $p\sigma$(C2s–C2p) and $s\sigma$(C2s–C2s) bondings of the main chain and of the C_6H_5. These $p\sigma$ and $s\sigma$ bondings correspond to the C–H and C–C regions for the spectra analysis of PE from MO calculations using n-$C_{13}H_{28}$ molecules based on the assignment of Delhalle et al.[18]

(b) Valence XPS of PVME, PVMK, PAA, PMA, PVAc, and PMMA Polymers. For the six polymers (Figs. 2, 3, 4, 5, 6, and 7), the theoretical spectra with the spectral patterns show good accordance with the experimental valence band spectra. The differences of the finger-print spectra between side chains (–OCH_3, –$COCH_3$, –COOH, –$COOCH_3$, –$OCOCH_3$, and –CH_3–C–$COOCH_3$ (PMMA)) of the polymers seem to be reflected in both the observed and simulated spectra. The shift due to work-function effects was obtained as 4.5, 3.5, and 3.0 eV for PVME and PVMK polymers, for three PAA, PMA, and PMMA polymers, and for PVAc, respectively.

In Figs. 2, 3, 4, 5, 6, and 7, the intense spectrum, which is due to an O2s-dominant contribution at around 27 eV, corresponds to the theoretical values of $s\sigma$(O2s–C2s)-bonding and $p\sigma$(O2s–C2p)-bonding orbitals. In this assignment of the polymers, which have both –O– and >C=O groups, for PVAc, the $s\sigma$ and $p\sigma$ orbitals result from the –O– and >C=O components, respectively. In the case of PAA, PMA, and PMMA, the $s\sigma$ and $p\sigma$ orbitals depend on two components, –O– and >C=O. Tables 3, 4, 5, and 6 show the orbital characters of the spectra for PVME, PVMK, PVAc, and PMA (similar tables for PAA and PMMA are omitted).

(c) Valence XPS of PAM, PNVP, and PMAM Polymers. Intense spectra between 20 and 30 eV for PAM, PNVP, and PMAM (Figs. 8, 9, and 10) were determined by both N2s and O2s main contributions, respectively. The peaks (at around 5 eV) are due to lone-pair orbitals of main-chain N and O for these polymers. We show the orbital characters of PAM and PNVP in Tables 7 and 8 (a similar table for PMAM is omitted). The shifts due to work-function effects were estimated to be 4.0, 4.5, and 5.0 eV for the trimer models of PAM,

Table 7. Observed Peaks, VIP, Main AO PICS, Orbital Nature and Functional Group for Valence XPS of PAM [(The Gap between Observed and Calculated VIPs)=4.0 eV]

Peak (eV)	VIP (eV)	Main AO PICS	Orbital nature[b)]	Functional group
27.0	30.77;30.45;30.22	O2s(0.8);N,C2s(0.1)	sσ(O2s–C2s)–B	O=C–,–C–NH_2
(25—32)[a)]				
22.5	27.67;27.38;27.12	N2s(0.6);O2s(0.4)	sσ(N,O2s–C2s)–B	H_2N–C–,O=C–
(17—25)[a)]	25.00;23.78;22.20	C2s	sσ(C2s–C2s)–B	–C–(main chain)
15.5	(20.47;19.83;	C2s	{sσ(C2s–H1s)–B;	{–C–(main chain),
	19.56)	C2s	pσ(C2s–C,N2p)–B}	–C–NH_2}
(12—17)[a)]	18.36;17.88;17.50	C2s	pσ(N,C2p–C2s)–B	–C–NH_2
	17.20;17.17;16.99	C2s(0.5);N2p(0.5)	pσ(N,C2p–C2s)–B	H_2N–C–
9.0	(13.18—13.01)	{O2s(0.5);C2p(0.3); O2p(0.2)}	pσ(O,C2p–O2p,2s)–B	O=C–C,–C–(main chain)
(6—12)[a)]	Many adjacent levels			
	(15.36—13.96)	C2p	pσ,pπ(C2p–C,N,O2p)–B	O=C–,H_2N–C–,–C–C–
	(12.62—10.93)	C2p(0.7),O2p(0.3)	pσ,pπ(O,C2p–2p)–B	–C–C=O
4.5	(9.39;9.10;9.06;	O2p;N2p	pπ(lone pair)–NB	–C=O,–NH_2
(3—6)[a)]	8.78;8.49;8.42)	O2p;N2p	pπ(lone pair)–NB	–C=O,–NH_2

a) Shows the peak range. b) B and NB mean bonding and nonbonding, respectively. (C,O2s–2p) means (C2s–C2p) and (O2s–O2p), (C2p, O2p–C2p) denotes (C2p–C2p) and (O2p–C2p), and so on.

Table 8. Observed Peaks, VIP, Main AO PICS, Orbital Nature and Functional Group for Valence XPS of PNVP [(The Gap between Observed and Calculated VIPs)=4.5 eV]

Peak (eV)	VIP (eV)	Main AO PICS	Orbital nature[b)]	Functional group
26.0	31.18;31.09;30.82	O2s(0.6);N,C2s(0.2)	sσ(O,N2s–C2s)–B	O=C,–N–C–
(21.5—30)[a)]	29.16;28.96;28.69	O2s(0.6);N2s(0.3)	pσ(O,N2s–C2p)–B	O=C,–N–C–
17.5	{22.48;22.28;	C2s(0.8);O2s(0.2)	sσ(C2s–C,O2s)–B	–C–C=O,–C–N–
	22.12;21.88}			
(16—21.5)[a)]	25.47;24.73;24.36	C2s	sσ(C2s–C2s)–B	–C–(main chain),–C–
	23.53;23.05	C2s(0.8);N2s(0.2)	sσ(C2s–C,N2s)–B	–C–(main chain),–CH_3
14.5	(19.56—19.09)	C2s	sσ,pσ(C2s–C2s,N2p)–B	–C–C–,–C–N–
(13—16)[a)]	20.54	C2s	sσ,pσ(C2s–C2s,N2p)–B	–C–C–,–C–N–
11.0	(17.30;16.99;	O2p(0.7);C2s(0.2)	pσ(C2p–C2s)–B	–C–N–,–C–C–
	16.75;16.74)			
(6—13)[a)]	Many adjacent levels			
	(16.56—11.12)	C2p,O2p,N2p	pσ,pπ(C,O,N2p–2p)–B	–C–C–,–C=O,–C–N–
4.0				
(2—6)[a)]	9.15;9.06;8.83	O2p(0.5);N2p(0.3)	pπ(lone pair)–NB	O=C–,–N–
	8.77;8.68;8.36	O2p(0.7);N2p(0.2)	pπ(lone pair)–NB	O=C–,–N–

a) Shows the peak range. b) B and NB mean bonding and nonbonding, respectively. (C,O2s–2p) means (C2s–C2p) and (O2s–O2p), (C2p, O2p–C2p) denotes (C2p–C2p) and (O2p–C2p), and so on.

PMAM, and PNVP, respectively. For these molecules, the spectra appeared to show good agreement with the observed ones when we used an approximate linewidth of 0.10 I_k.

It is very interesting that we could observe the characteristic spectra due to the PICS for any atomic orbital of the constituent elements of the functional groups. For these ten polymers, we have clarified the orbital nature of the finger-print spectra, which were characterized from the constituent elements (C, N, and O) in the range of 0—30 eV.

(d) Spectral Linewidths of Valence XPS for Polymers. As mentioned in a previous paper,[19] the spectral linewidths below 12 eV are determined by broadening due to many adjacent MO energy levels. By contrast, the linewidths in the range of 13—30 eV may be governed by a relaxation of the inner-valence 2s electron states for the MO levels. In this section, since the linewidths of O2s, or the N2s spectra of the polymers were obtained as 2.5—4.0 eV, we describe the reason for the broadening.

The broadening of the inner-valence bands is due to the same reason as for gas-phase single molecules: A breakdown of the one-particle picture accompanying shake-up phenomena. The foot and wing of the broader peak of the inner-valence ionization results from a transition which was considered as being a mixing between single ionization and simultaneous ionization–excitation (shake-up) configurations.[10,12,27—30]

For polymers, we obtained additional broadening due

to neighboring MO levels. We, then, parameterized the linewidth ($WH(k)$) as an arbitrary value of 0.10 I_k, since the state of each MO level has an individual electronic relaxation. A good fit between our simulation and the observed spectra of polymers seems to confirm that our general interpretation is not unreasonable.

References

1) L. Åsbrink, C. Fridh, and E. Lindholm, *Chem. Phys. Lett.*, **52**, 63 (1977); *Quantum Chem. Program Exchange*, **12**, No. 398 (1980).

2) L. Åsbrink, C. Fridh, and E. Lindholm, *Chem. Phys. Lett.*, **52**, 69 (1977).

3) E. Lindholm and L. Åsbrink, "Molecular Orbitals and Their Energies, Studied by the Semiempirical HAM Method," Springer-Verlag, Berlin (1985).

4) J. C. Slater, *Phys. Rev.*, **36**, 57 (1930).

5) J. C. Slater, "Quantum Theory of Atomic Structure," McGraw-Hill, New York (1960), Vol. 1, p. 368.

6) J. C. Slater, *Adv. Quantum Chem.*, **6**, 1 (1972).

7) D. P. Chong, *Theor. Chim. Acta*, **51**, 55 (1979).

8) D. P. Chong, *J. Mol. Sci.*, **2**, 55 (1982).

9) D. P. Chong, *Chem. Phys. Lett.*, **82**, 511 (1981).

10) D. P. Chong, *Can. J. Chem.*, **61**, 1 (1983).

11) A. Gardner, P. K. Mukherjee, and D. P. Chong, *J. Mol. Struct. Theochem.*, **108**, 25 (1984).

12) D. P. Chong, *Can. J. Chem.*, **63**, 2007 (1985).

13) D. S. Urch, L. Bergknut, T. K. L. M. Young, R. S. Kim, and D. P. Chong, *Spectrosc. Lett.*, **13**, 487 (1980).

14) P. Boulanger, C. Magermans, J. J. Verbist, J. Delhalle, and D. S. Urch, *Macromolecules*, **24**, 2757 (1991).

15) P. Boulanger, R. Lazzaroni, J. J. Verbist, and J. Delhalle, *Chem. Phys. Lett.*, **129**, 275 (1986).

16) S. R. Cain, *Chem. Phys. Lett.*, **143**, 361 (1988).

17) P. Boulanger, J. Riga, J. J. Verbist, and J. Delhalle, *Macromolecules*, **22**, 173 (1989).

18) J. Delhalle, S. Delhalle, and J. Riga, *J. Chem. Soc., Faraday Trans. 2*, **1987**, 503.

19) K. Endo, N. Kobayashi, M. Aida, and C. Inoue, *J. Phys. Chem. Solids*, **54**, 887 (1993).

20) K. Endo, C. Inoue, N. Kobayashi, T. Higashioji, and H. Nakatsuji, *Bull. Chem. Soc. Jpn.*, **66**, 3241 (1993).

21) K. Endo, C. Inoue, N. Kobayashi, and M. Aida, *J. Phys. Chem. Solids*, **55**, 471 (1994).

22) K. Endo, Y. Kaneda, M. Aida, and D. P. Chong, to be published.

23) U. Gelius and K. Siegbahn, *Faraday Discuss. Chem. Soc.*, **54**, 257 (1972); U. Gelius, *J. Electron Spectrosc. Relat. Phenom.*, **5**, 985 (1974).

24) P. H. Citrin, R. W. Shaw, Jr., A. Packer, and T. D. Thomas, "Electron Spectroscopy," ed by D. A. Shirley, North-Holland Publishing Co., Amsterdam (1972), pp. 691—706.

25) J. J. P. Stewart, *J. Comput. Chem.*, **10**, 289 (1989).

26) V. I. Nefedov, N. P. Sergushin, I. M. Band, and M. B. Trzhaskovskaya, *J. Electron Spectrosc. Relat. Phenom.*, **2**, 383 (1973).

27) J. Duffy and D. P. Chong, *Org. Mass Spectrom.*, **28**, 321 (1993).

28) H. Nakatsuji and T. Yonezawa, *Chem. Phys. Lett.*, **87**, 462 (1982).

29) H. Nakatsuji, *Chem. Phys.*, **75**, 425 (1983).

30) H. Nakatsuji, *Chem. Phys.*, **76**, 283 (1983).